Article

Inhibitors of the Diadenosine Tetraphosphate Phosphorylase Rv2613c of Mycobacterium tuberculosis

Kathrin H. Götz, Stephan M. Hacker, Daniel Mayer, Jan-Niklas Dürig, Steffen Stenger, and Andreas Marx

ACS Chem. Biol., **Just Accepted Manuscript** • DOI: 10.1021/acschembio.7b00653 • Publication Date (Web): 11 Sep 2017

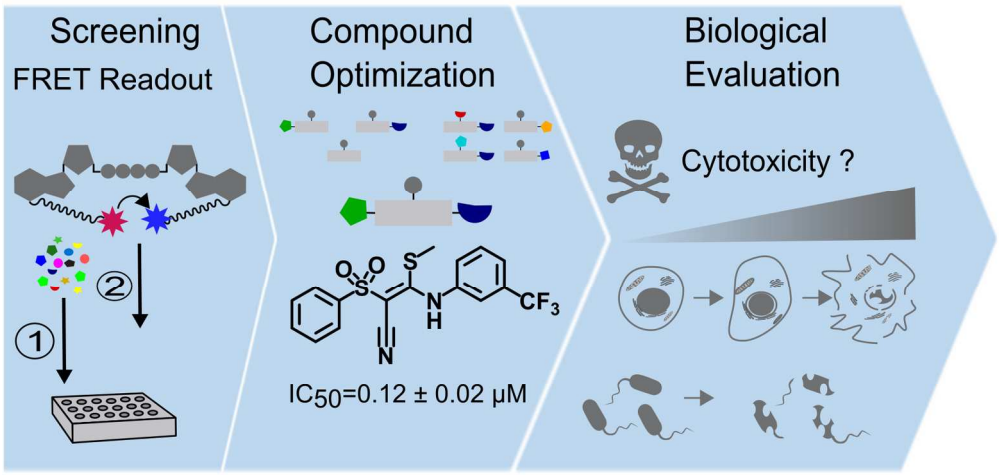

Table of Content graphic

500x240mm (96 x 96 DPI)

Inhibitors of the Diadenosine Tetraphosphate Phosphorylase Rv2613c of *Mycobacterium tuberculosis*

Kathrin H. Götz[‡], Stephan M. Hacker[‡], Daniel Mayer[†], Jan-Niklas Dürig[‡], Steffen Stenger[†], Andreas Marx[‡*]

[‡] Department of Chemistry, Konstanz Research School Chemical Biology, University of Konstanz, Universitätsstrasse 10, D-78464 Konstanz, Germany

[†] Institute for Medical Microbiology and Hygiene, University Hospital of Ulm, Albert-Einstein-Allee 11, D-89081 Ulm, Germany

M. tuberculosis, diadenosine tetraphosphate, diadenosine tetraphosphate phosphorylase, Rv2613c, FRET, High Throughput Screening

ABSTRACT: The intracellular concentration of diadenosine tetraphospate (Ap_4A) rises upon exposure to stress conditions. Despite being discovered over 50 years ago, the cellular functions of Ap_4A are still enigmatic. If and how the varied Ap_4A is a signal and involved in the signaling pathways leading to an appropriate cellular response, remains to be discovered. As the turnover of Ap_4A by Ap_4A cleaving enzymes is rapid, small molecule inhibitors for these enzymes would provide tools for the more detailed study of the role of Ap_4A. Here, we describe the development of a high-throughput screening assay based on a fluorogenic Ap_4A substrate for the identification and optimization of small molecule inhibitors for Ap_4A cleaving enzymes. As proof-of-concept we screened a library of over 42,000 compounds towards their inhibitory activity against the Ap_4A phosphorylase (Rv2613c) of *M. tuberculosis* (*Mtb*). A sulfanylacrylonitril derivative with an IC_{50} of 260 ± 50 nM *in vitro* was identified. Multiple derivatives were synthesized to further optimize their properties with respect to their *in vitro* IC_{50} values and their cytotoxicity against human cells (HeLa). In addition we selected two hits to study their anti-mycobacterial activity against virulent *Mtb* to show that they might be candidates for further development of antimycobacterial agents against multi drug resistant *Mtb*.

Diadenosine tetraphosphate (Ap_4A) was discovered in the middle of the 1960s[1]. It consists of two adenosine moieties, which are linked by four phosphates via phosphoanhydride bonds that are esterified with the 5'-hydroxyl groups (Figure 1). Ap_4A is found in prokaryotic as well as eukaryotic cells[2]. Cellular concentrations vary depending on cell type and environmental factors, such as pH, temperature and oxidants[3-5], from the nanomolar to the millimolar range[1, 3, 5-7]. An increase of intracellular Ap_4A concentrations is observed upon stress[4, 8, 9]. Therefore, it was postulated that Ap_4A serves as cellular signal ('alarmone') of stressors and is thus involved in the adaptive processes of cells to these conditions. However, the exact role and mechanisms *in vivo* are yet to be specified. The intracellular level of Ap_4A is determined by its synthesis and degradation. The major synthesis path *in vivo* is believed to be a side reaction of the amino acid activation, which is catalyzed

by various aminoacyl tRNA synthetases (aaRS)[10]. During this process aminoacyl-AMP (aaAMP) is formed, which can be either attacked by its cognate tRNA to form aminoacyl-tRNA or by ATP to form Ap_4A[11]. It was postulated by Lee *et al.* that tRNAs could be the sensors of stress conditions and cause appropriate tRNA synthetases to synthesize more Ap_4A in response to changes in tRNA modified nucleotides[7] thereby linking the cellular stress response to Ap_4A synthesis.

Three classes of enzymes are known to catalyze the degradation of Ap_4A[12]: symmetrically cleaving Ap_4A hydrolases that form two molecules of adenosine diphosphate (ADP), which are found in lower organisms such as primitive eukaryotes (*e.g.* slime mold) and prokaryotes (*e.g. E. coli*)[13], asymmetrically cleaving Ap_4A hydrolases that form one molecule of adenosine triphosphate (ATP) and one molecule of adenosine monophosphate (AMP), which mainly exist in higher eukaryotes such as humans[1], as well as Ap_4A phosphorylases, which occur in very few organisms including *M. tuberculosis* (*Mtb*)[14] (Figure 1).

Assays that allow studying the enzymatic activity of these diverse catabolic enzymes for Ap_4A could largely help to better understand and eventually modulate the functions of Ap_4A in various organisms. In a mutagenesis study by Sassetti *et al.* it was shown that the Ap_4A phosphorylase (Rv2613c, Figure 1) of *Mtb* is an essential gene for the optimal growth and proliferation of the bacteria[14]. If Rv2613c' function is impaired Ap_4A, which is constantly formed as by-product in low quantities[10], accumulates and the cells experience a constant stress response impairing their growth and proliferation. It is worth attention, that Rv2613c has no human analog[11, 15].

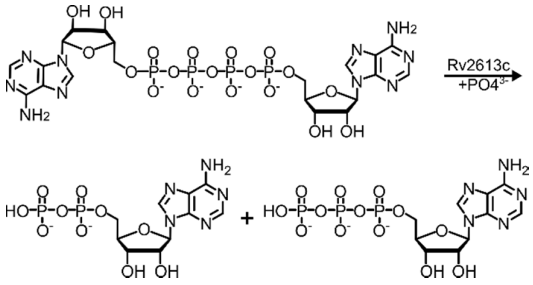

Figure 1 Enzymatic activity of the Ap_4A phosphorylase Rv2613c cleaving Ap_4A into ADP and ATP.

This enzyme might therefore be an attractive target for drugs targeting *Mtb* without affecting the function of human cells. Therefore, we chose Rv2613c as a model system to establish an activity assay for Ap_4A phosphorylases. To be able to monitor the enzymatic activity of Rv2613c in high throughput, we developed the fluorogenic Ap_4A analogue **1** (Figure 3A). Based on a recently developed concept to study a variety of nucleotide-dependent processes[16-21], this analogue contains two fluorophores that are able to undergo Förster resonance energy transfer (FRET). After enzymatic cleavage of the phosphate chain FRET is no longer possible resulting in a profound change of fluorescence characteristics (Figure 3B, Figure S2). Using this analogue as a tool, we performed a high throughput screen of more than 42,000 compounds. The most promising initial hit was optimized to yield potent small molecule inhibitors of Rv2613c *in vitro* with low cytotoxicity against human cells. Furthermore, two compounds were studied towards their anti-mycobacterial activity against virulent *Mtb* to show that they are candidates for further development of antimycobacterial agents against multi drug resistant *Mtb*.

RESULTS AND DISCUSSION

Design of the Probe and Screening

To analyze the binding of Ap_4A in the active site of Rv2613c, docking studies with the crystal structure of Rv2613c were performed using the program SwissDock[22, 23] (Figure 2). The fluorogenic Ap_4A analogue **1** (Figure 3A) was chosen based on the docking results, which show that both N^6 positions should be accessible for modifications (Figure 2B). **1** was synthesized in 7 steps in analogy to reported procedures[16, 21]. We found that Rv2613c is able to process **1** in an

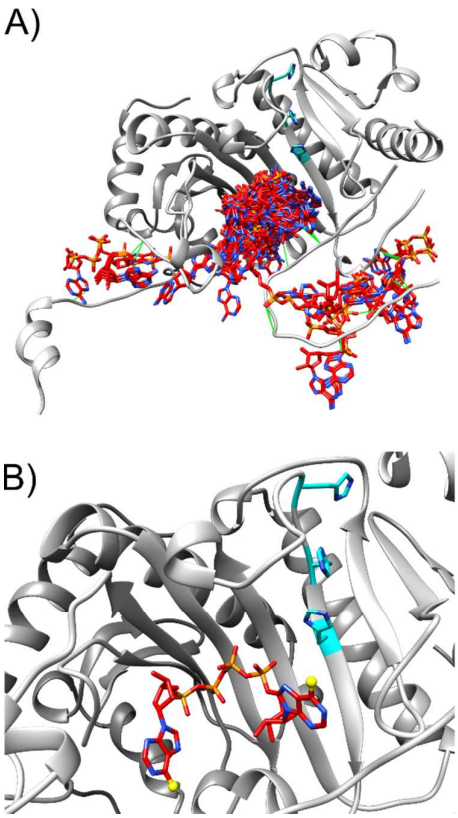

enzyme-concentration dependent manner (Figure S1, Figure S2) resulting in a shift of the fluorescence maxima from 662 nm to 563 nm upon cleavage (Figure 3B). The fluorescence spectrum of a solution of **1** in the presence of Rv2613c shows a decrease of the acceptor fluorescence over time accompanied by an increase of the donor fluorescence intensity. The donor fluorescence intensity is therefore used as a measure for the cleavage of **1**. In the absence of enzyme, the fluorescence signal is unaltered over time (Figure S1, Figure S2A). Using this change in fluorescence intensity as readout for enzymatic activity, we screened more than 42,000 small molecules for their inhibition of Rv2613c. The general procedure of the assay is depicted in Figure 3C. Briefly, the compounds of the library dissolved in DMSO were added to Rv2613c. Controls were performed by addition of DMSO to reactions with and without the enzyme. The fluorescence intensities were

measured directly after addition of **1** and after 30 minutes incubation. The difference between the two values was defined as Rv2613c activity.

Figure 2 Docking model using the crystal structure of Rv2613c (PDB ID: 3ANO, grey) with Ap_4A (red). The modeling was performed with the SwissDock web service[22, 23] A) All obtained results docking Ap_4A (red) into Rv2613c B) Best model according to SwissDock (Cluster 0 Element 0) with zoom into the binding site of Rv2613c. Active site histidine residues (His 151, His 153, His 155) are shown as cyan sticks. The yellow balls indicate the positions of modification at the N^6-position for the FRET analogue **1**.

This excludes effects of inherently fluorescent compounds or compounds that quench fluorescence. From this value, inhibition by each compound relative to the controls was calculated. Results were analysed using the KNIME Analytics platform[24]. As a quality control Z'-values were calculated for every multiwell plate and were consistently larger than 0.85[25] demonstrating the high reproducibility of the assay. Compounds were defined as hits, if the residual activity was 50% or lower. Applying these criteria we identified 21 molecules with inhibitory potential (Table S1). Methylsulfanylacrylonitril **2** (Figure 3D) was the most promising hit of the initial screening. It showed more than 98% inhibition at 10 µM concentration. This potency directly from the screening deck made this compound a very interesting starting point for further investigation.

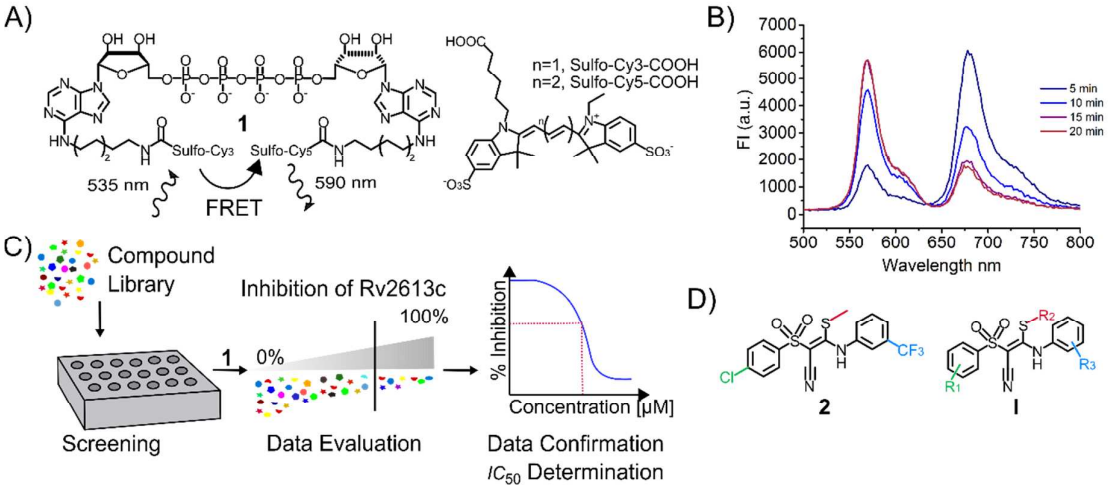

Figure 3 A) Doubly labelled Ap_4A FRET probe **1**. B) Time-dependent change of the fluorescence spectra upon treatment of a solution of probe **1** in the presence of Rv2613c. Fluorescence measurements were performed with excitation at 490 nm over 20 min. C) General outline of the high throughput screening assay. Compound libraries were screened, the data was evaluated by KNIME[24], followed by data conformation, further biological evaluation and compound optimization. D) Methylsulfanylacrylonitril (**2**) was the most promising compound detected by the screening. It showed more than 98% inhibition at 10 µM concentration. In scaffold **I** are three substituents indicated that were investigated towards their influence on the inhibitory effect on Rv2613c activity and cytotoxicity against HeLa cells.

Synthesis of Sulfanylacrylonitriles

In order to verify the activity of **2**, the compound was synthesized along with some structural analogues (Figure 4). The synthesis of compounds of this class comprises 5 steps in total and allows to synthesize a diverse set of derivatives using commercially available starting materials. The substituted aryl sulfonyl acetonitriles (**V**) were synthesized in two steps starting from the substituted aryl thiols (**II**). The substitution reaction with bromoacetonitrile (**III**) was carried out under mild basic conditions (K_2CO_3) in DMF at 0 °C for 2 - 3 h. The intermediate aryl sulfide acetonitriles (**IV**) could be isolated as a crude product and were dried before oxidation to the sulfonyl acetonitriles (**V**) in DCM with *m*CPBA at 0 °C for 2 h[26]. The crude products were recrystallized from EtOH to yield the respective sulfonyl acetonitriles (**IV**) as colourless crystals in moderate to high yields. For the synthesis of the respective isothiocyanates (**VII**), the modified anilines (**VI**) were reacted with thiophosgene in the presence of NEt_3 in dry THF at 0 °C for 2 h.[27] The desired isothiocyanates (**VII**) were purified by flash column chromatography in moderate yield. Coupling of the respective sulfonyl acetonitrile (**V**) with the isothiocyanate (**VII**) was performed in dry acetone under mild basic conditions (K_2CO_3) in an inert atmosphere at room temperature for 2 h[28, 29]. After completion of the reaction K_2CO_3 was removed by filtration and the sulphur instantly alkylated by the addition of the respective alkyl halogenide[28, 29]. The reaction mixture was stirred for 2 h at room temperature. After recrystallization of the crude product from EtOH the desired alkylsulfanylacrylonitrils **I** were obtained in moderate to high yields. In this way, 21 compounds (**2**-**22**) were synthesized (Table 1).

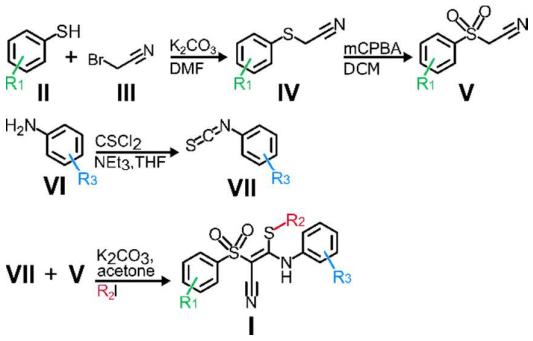

Figure 4 General synthesis of alkyl-sulfanylacrylonitril derivatives **I.**

Evaluation of the Sulfanylacrylonitrile Derivatives

The developed assay was utilized to evaluate the relative inhibitory potential of the compounds by determining IC_{50} values of all 21 compounds (**2**-**22**, Table 1). For this purpose, the assay was performed as described above. Time points were taken every 3 minutes to closely monitor the enzymatic reaction. Desired molecules should ideally combine high enzymatic activity and low cytotoxicity against eukaryotic cells. This might ideally allow studying intracellular *Mtb* without affecting their host cells. Therefore, we also tested all compounds for their cytotoxicity against a human epithelial cell line (HeLa cells) with a colorimetric assay, which determines the metabolic activity of cells, and thus their viability. The viability is measured as a function of the reduction of the tetrazolium dye 3-(4,5-dimethylthiazol-2-yl)-2,5-diphenyltetrazolium bromide (MTT) into insoluble formazan by NAD(P)H- dependent oxidoreductases[30].

The resynthesized compound **2** potently inhibited Rv2613c activity with an IC_{50} of 257 ± 52nM. However, compound **2** is highly cytotoxic against HeLa cells (EC_{50} of 3.05 ± 0.86 µM). Therefore, we set out to optimize **2** for reduced cytoxicity and further enhanced enzymatic activity. The

scaffold of **2** shows three substituents (compare Figure 3D, **I**), which can be easily manipulated. Following the general synthesis (Figure 4) several derivatives of the initial hit **2** were synthesized to elucidate the influence of the three substituents.

First, we elucidated the role of the two substituents of the phenyl rings (R_1 and R_3). For this purpose derivatives **3**-**5** were synthesized. The unsubstituted analogue **3** (R_1=R_3=H) as well as compound **4** bearing only the modification at R_1 were inactive. Both compounds showed also a drastically reduced cytotoxicity towards HeLa cells. Compound **5** (R_1=H, R_3=CF_3) exhibited comparably strong inhibition as the initial hit **2** and at the same time a lower cytotoxicity (EC_{50} = 13.3 ± 4.5 µM). Since this showed that the R_1-substituent has no significant effect on the activity, the unsubstituted sulfonylacetonitril (R_1=H) was used in the synthesis for further derivatives.

Table 1 Overview of all synthesized sulfanylacrylonitril derivatives (**2**-**22**). Indicated are the three substituents (Figure 3D, **I**) and the IC_{50} values of the FRET assay and the EC_{50} values against HeLa cells with their respective standard deviations.

	R_1	R_2	R_3	FRET IC_{50} [µM]	Cytotoxicity EC_{50} [µM] [HeLa]
2	-Cl	-Me	-*m*-CF_3	0.26 ± 0.05	3.05 ± 0.86
3	-H	-Me	-*m*-H	>30	>100
4	-Cl	-Me	-*m*-H	>100	>30
5	-H	-Me	-*m*-CF_3	0.12 ± 0.02	13.3 ± 4.49
6	-H	-Me	-*o*-CF_3	>100	<0.05
7	-H	-Me	-*p*-CF_3	16.3 ± 4.9	23.4 ± 7.1
8	-H	-Me	-2x-*m*-CF_3	>100	>100
9	-H	-Et	-*m*-CF_3	1.82 ± 0.48	5.43 ± 2.24
10	-H	-*n*Pr	-*m*-CF_3	0.47 ± 0.06	1.47 ± 0.61
11	-H	-*i*Pr	-*m*-CF_3	0.94 ± 0.26	7.10 ± 3.05
12	-H	-Bz	-*m*-CF_3	0.80 ± 0.21	1.00 ± 0.59
13	-H	-All	-*m*-CF_3	1.47 ± 0.10	3.30 ± 2.40
14	-H	-Me	-*m*-Me	4.62 ± 0.76	>100
15	-H	-Me	-*m*-NO_2	1.30 ± 0.46	<0.140
16	-H	-Me	-*m*-CN	2.51 ± 0.91	2.31 ± 1.34
17	-H	-Me	-*m*-COOMe	21.8 ± 3.6	5.67 ± 3.35
18	-H	-Me	-*m*-Et	0.57 ± 0.17	>30
19	-H	-Me	-*m*-Pr	0.96 ± 0.15	26.3 ± 21.0
20	-H	-Me	-*m*-iPr	1.77 ± 0.20	18.2 ± 7.1
21	-H	-Me	-*m*-OMe	11.3 ± 2.7	>30
22	-H	-Me	-2x-*m*-CH3	>100	>100

Next, we investigated, if the position of the CF_3 group at R_3 influences the inhibitory potential of the compound. It was found, that multiple substitution in *meta*-position

(**8**) and substitution in *ortho*-position (**6**) lead to inactive compounds in regards to Rv2613c inhibition. Substitution in *para*-position (**7**) leads to a drastic decrease in the inhibitory potential, while having cytotoxicity comparable to **5**. Whereas **8** exhibited no detectable cytotoxicity (EC_{50} >100 µM), **6** was very cytotoxic (EC_{50} <0.05 µM). Modification in one of the *meta*-positions with an R_3 group is therefore necessary for compound activity. Additionally, the influence of the alkyl substituent at the thiol residue (R_2) was studied while keeping the other positions unaltered (R_1=H, R_3=*m*-CF_3) (**9**-**13**). For this purpose, the alkylating agent was altered. Instead of using methyl iodide other alkyl halogenides were used (R_2=Et, *n*Pr, *i*Pr, Bn, allyl). We found that the alteration of the alkyl substituent has little influence on the inhibitory potential towards Rv2613c with 50% inhibition at concentrations ranging between 0.40 - 1.82 µM (compare Table 1). The fact, that the sterically demanding benzyl substituent (**12**) is accepted as well as a methyl group (**5**) indicates that this substituent is not crucially involved in the interaction with the enzyme. The cytotoxicity of compounds **9**-**13** was also in the lower µM range, and thereby somewhat lower in comparison to **5**.

Taken together, changes of the R_3 group in the *meta*-position of that phenyl ring seemed most promising to further optimize the compounds in regard to a high potency against Rv2613c and low cytotoxicity towards human cells.

Since the CF_3 group used so far in the R_3 position is an electron-withdrawing group we investigated next, if this is a necessary trait for a compound with inhibitory potential against Rv2613c. For this purpose analogues **14**-**17** were synthesized. Analogue **14** contains a methyl substitution that has no electron withdrawing properties, but approximately the same steric demand as the CF_3 group. Analogues **15**-**17** bear various substitutions with electron withdrawing properties (R_3=NO_2, CN, CO_2Me). All analogues with altered electron withdrawing groups display increased cytotoxicity, and simultaneously decreased inhibition of Rv2613c (Table 1). In contrast compound **14** showed a strong decrease in cytotoxicity (EC_{50} >100 µM) but retained considerable inhibitory potential (IC_{50}= 4.62 ± 0.76 µM). Having an electron-withdrawing group at the R_3-position is therefore not essential for compound activity and an electroneutral substituent at this position seems to be useful for optimizing the toxicity profile.

Due to the favorable activity and toxicity of **14**, we examined different alkyl substitutions in the *meta*-position more closely. In order to do this, analogues **18**-**22** were synthesized. The compounds generally show an increasing cytotoxicity with elongation of the alkyl substituent in meta-position (Me < Et < *i*Pr ≤ OMe < *n*Pr). Analogue **18** (R_3=Et) has the best inhibitory potency with an IC_{50} of 0.57 ± 0.17 µM. Compound **19** (R_3=*n*Pr) and **20** (R_3=*i*Pr) also have an improved inhibitory potency compared to the Me analogue (**14**). Derivative **21** (R_3=OMe) was less effective. Overall compounds **5** and **18** exhibit the best properties regarding the efficient inhibition of Rv2613c and limited cytotoxicity against human HeLa cells. The respective dose response curves for the FRET assay as well as for the MTT assay are shown in Figure S4. For **5** the EC_{50} for cytotoxicity is over 150 times higher than the IC_{50} *in vitro*, for **18** this ratio is lower but with over 100 times still gives a reasonable window to study Rv2613c function

To analyze its stability, compound **5** was incubated in a mixture of d_6-DMSO and phosphate buffered saline over 8 days at room temperature. The NMR spectra was unaltered during this time, revealing the

high stability of **5** in aqueous buffer (Figure S6).

To verify that the inhibitory effect also applies when the natural substrate Ap_4A is processed, the most promising compounds were evaluated towards their inhibition of the turnover of unmodified Ap_4A by Rv2613c. For this purpose, we determined Ap_4A cleavage by analytical HPLC in the presence of different sulfanylacrylonitrile derivatives or DMSO (Figure 5A). The IC_{50} of **5** for the natural substrate is 0.16 ± 0.01 µM and therefore similar to that measured with the FRET probe. Compound **18** displays with 3.11 ± 0.26 µM a slightly higher IC_{50} value indicating that the modifications in probe **1** might alter processing of compound **18**.

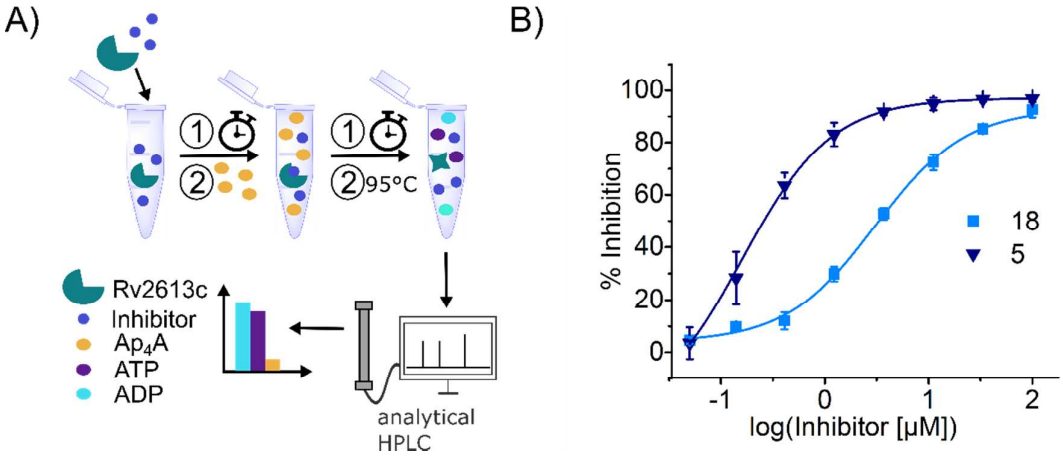

Figure 5 A) General outline of a HPLC-based assay for investigation of cleavage of natural Ap_4A. Rv2613c is preincubated for 30 min at 25°C with the inhibitor or DMSO as control in a phosphate containing buffer. Natural Ap_4A is added and the reaction is incubated at 25°C for another 60 min. During this time Rv2613c cleaves Ap_4A by phosphorolysis into ATP and ADP. Next the enzyme is inactivated and the reaction mixture is separated by analytical RP-HPLC. The different nucleotide species are quantified, and inhibition is calculated relative to the DMSO control. B) Dose response curves *in vitro* against Rv2613c with unmodified Ap_4A as the substrate for derivatives **5** and **18**. The IC_{50} value are determined as 0.16 ± 0.01 µM for compound **5** and as 3.11 ± 0.26 µM for compound **18.**

These results demonstrate that our screening system allows the detection of compounds, which are able to inhibit Rv2613c in the presence of the natural Ap_4A as a substrate.

Prediction of the Binding Mode

To gain insights whether the sulfanylacrylonitrile derivatives inhibit Rv2613c in a competitive manner by binding to the active site or by an allosteric effect, docking studies were performed using the SwissDock webservice[22, 23]. The docking was performed with both isomers (E-/Z-) of **5,** since the electron withdrawing properties of the phenyl-SO_2 moiety decreases the rotation barrier at the double bound, so that rotation and thereby transition from E to Z and *vice versa* is possible at low temperatures[31]. Both models were compared to a model

docking of Ap_4A which shows that Ap_4A mainly binds in a pocket near the active site histidine residues (Figure 2A).The E-Isomer and the Z-Isomer respectively bind in 73% and 65% of the cases in the Ap_4A binding site (Figure S7). Hence, the data indicates that **5** binds to the active site and should be competitive towards the natural substrate. Comparing the E- and Z-configurations a trend towards preferred binding of the E-isomer is suggested (Figure S7). Since all sulfanylacrylonitrile derivatives are structurally similar, we assume that they possess the same binding mode.

Inhibition of Metabolic Activity of *Mtb* by Sulfanylacrylonitril Derivatives

Based on the profound inhibition of the essential enzyme Rv2613c combined with the limited toxicity against human cells, we selected compounds **5** and **18** for evaluating the antimicrobial activity against virulent *Mtb*. To measure the metabolic activity of *Mtb* we measured the uptake of ^{3}H-uracil as described, since this assay was used in earlier studies of measuring activity of small molecules acting against *Mtb*[32]. Compounds **5** and **18** were tested in three different concentrations (1000, 100, and 10 µM). Untreated cells, as well as cells treated with diluent only (0.75% DMSO) served as controls. Both compounds (**5**, **18**) showed significant anti-mycobacterial activity at 1 mM (358 µg/mL, 398 µg/mL), concentration. Compound **18** reduced the uracil-uptake by 33 (± 12)%, while compound **5** was slightly less active (Figure 6B). At the same time rifampicin (2.43 µM, 2 µg/mL), a first-line anti-TB drug[33], which served as control, is more active reducing uracil uptake by 65 (± 19)%. Rifampicin

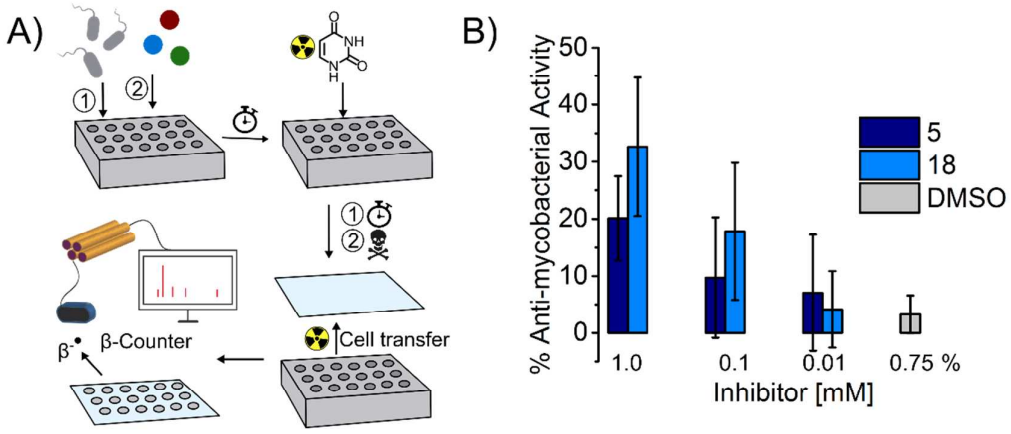

Figure 6 A) General outline of the ^{3}H-uracil proliferation assay to study toxicity towards *Mtb*. *Mtb* is seeded into a multiwall plate, **5** and **18** are added, respectively, and the plate is incubated for 2 h at 37°C. ^{3}H-uracil is added and the plate is incubated for 18 h at 37°C. Afterwards *Mtb* are inactivated by addition of 4% paraformaldehyde. The cells are transferred onto a glass fiber filter and after addition of a scintillant the radioactivity is measured using a β-counter. B) Anti-mycobacterial activity of compounds **5** and **18** in % at three different concentrations and 0.75% DMSO as control. Depicted is the mean of six independent experiments. The error bars represent the standard deviation over those six experiments.

targets the β subunit of the bacterial RNA-polymerase[34]. Hence, direct comparison with the sulfanylacrylonitrile derivatives might be questionable. Since Rv2613c, is involved in stress response, inhibiting its function might have greater impact, if the cells already experience stress *e.g.* if other antibiotics are present in combination therapy.

CONCLUSION

Taken together, we developed a high-throughput assay for the identification of inhibitors for Ap_4A cleaving enzymes. We utilized an Ap_4A analogue (**1**) modified with two fluorescent dyes, able to undergo FRET. Cleavage of the substrate induces a significant change of fluorescence, directly correlating with enzyme activity. Exploiting this tool, we screened more than 42,000 small molecules for inhibition of the Ap_4A phosphorylase Rv2613c of *Mtb*. Identifying sulfanylacrylonitril derivative **2** as an inhibitor with sub-micromolar potency. We verified the inhibitory potential of this compound using chemical synthesis. However, compound **2** demonstrated strong cytotoxicity against human cells thereby limiting its potential for applications in host cells. We therefore optimized the scaffold of the molecule using the developed assay to guide compound development and synthesized highly effective molecules inhibiting Rv2613c with little toxicity against a human cell line. With these optimized compounds in hand, it will now be possible to study the role of Ap_4A and the enzymatic activity of Rv2613c in more detail and under various conditions *e.g.* extra- and intracellular *Mtb*. Since two selected derivatives also demonstrated activity against virulent *Mtb* they could be starting points for a new class of anti-mycobacterial drugs. These compounds could also be the basis for the development of semisynthetic bioluminescent sensors to measure concentrations of Ap_4A in cells and to verify target engagement in cells[35, 36 37]. Noteworthy, the underlying concept of the herein depicted high-throughput assay might be further exploited for the identification of small molecule inhibitors for other Ap_4A cleaving enzymes.

METHODS

High-throughput Screening of Inhibitors for Rv2613c

For the fully automated screening, a Freedom evo screening unit (TECAN) was used. Rv2613c which was recombinantelly expressed in *E. coli* (Supporting Information) was diluted to 2.0 nM in buffer containing 20 mM Tris-HCl (pH 8.0), 50 mM NaCl, 1 mM DTT and 0.2 mg/mL BSA. 50 µL of this solution were dispensed into all wells of columns 1 to 23 of a 384 well plate (PS, flat bottom, black, non-binding, Greiner Bio-one) using the multichannel arm (MCA) and a MCA 384 adapter for disposable tips (DiTis, 125 µL, TECAN). Column 24 of the plate was filled with 50 µL of the same buffer without enzyme using the 4 channel liquid handling arm (LiHa, Ditis, 200 µl, TECAN). 10 µM of the compounds of the library dissolved in DMSO were transferred into the plate using the MCA with a 384 fixed tips tool (15 µl, TECAN). DMSO was transferred into column 23 and column 24 (control). The reactions were incubated at 25°C for 30 min. Probe **1** (1.33 µM) was dissolved in buffer containing 20 mM Tris-HCl (pH 8.0), 50 mM NaCl, 5 mM $MgCl_2$ and 5 mM NaH_2PO_4. 30 µL of this solution were added to the reactions using a Multidrop 384 reagent dispenser (Thermo Scientific). The fluorescence intensity was immediately measured in all wells using fluorescence excitation at 535 nm and detection of the fluorescence emission at 590 nm in an infinite F500 plate reader (TECAN). The reactions were incubated

for 30 min at 25°C and the fluorescence intensity was measured again using the same excitation and emission wavelengths. Relative enzymatic activity was calculated as the difference of the two fluorescence intensity measurements for the same well. This value was used to calculate inhibition by each compound relative to the controls on the same plate. Data was analyzed using the KNIME Analytics platform[24]. As a quality control Z'-values were calculated for every plate[25]. Compounds were defined as hits, if the inhibition was above 50%.

Assay for Measuring Rv2613c Inhibition by FRET

To conduct this assay, a black, coated, non-binding 384 well microplate (Greiner bio-one) was used. In each well, 59.2 µL mastermix (8 nM Rv2613c in 20 mM Tris-HCl (pH 8.0), 50 mM NaCl, 1 mM DTT, 0.2 mg/mL BSA, 5 mM NaH_2PO_4, 5 mM $MgCl_2$) and 0.8 µL of inhibitor (indicated concentrations) in DMSO were mixed. One control column without enzyme (59.2 µL Tris-HCl buffer (20 mM Tris-HCl (pH 8.0), 50 mM NaCl, 1 mM DTT, 0.2 mg/mL BSA, 5 mM NaH_2PO_4, 5 mM $MgCl_2$) and 0.8 µL of each 10 mM inhibitor in DMSO and one control row without inhibitor but 1% DMSO instead (59.2 µL mastermix (8 nM Rv2613c in 20 mM Tris-HCl (pH 8.0), 50 mM NaCl, 1 mM DTT, 0.2 mg/mL BSA, 5 mM NaH_2PO_4, 5 mM $MgCl_2$ and 0.8 µL DMSO) were added. After centrifugation (800 rpm, 5 sec.) the plate was incubated at 25°C for 30 min, followed by addition of substrate **1** (20 µL each well, 2 µM in Tris-HCl buffer pH 8.0). Measurement of the fluorescence at 570 nm was conducted using an infinite F500 plate reader (TECAN) every 3 min over one hour. Turnover of probe **1** was calculated by normalization to the intensity for products and non-cleaved probe **1** under the same conditions. The rate of probe **1** turnover was obtained by linear fitting of probe **1** turnover over time. % Inhibition was calculated relative to the controls. The IC_{50} was calculated by a non-linear curve fit/dose response curve in Origin®[38]. All data represent mean standard error of triplicates.

MTT-based Cytotoxicity Assay

In each well of a 96-well plate, 170 µL of DMEM (Dulbecco's Modified Eagle's medium + FCS + PenStrep) and 30 µL of a confluent 10 cm culture plate of HeLa cells trypsinized into 10 mL of DMEM were pipetted. The plate was stored in an incubator (5% CO_2) at 37°C overnight. 2 µL of each inhibitor at the indicated concentration were added and incubated for 24 h at 37°C. Cells treated with 1% DMSO instead of an inhibitor and medium without cells and 1% DMSO served as controls. MTT (5 mg/mL in water) was diluted with DMEM in a 1:10 ratio and 100 µL were added into each well. After 1 h incubation at room temperature, the medium was removed and 100 µL of DMSO were added. The plate was incubated at room temperature on a shaker until the crystals were fully dissolved. Absorbance was measured using a 1420 multilable counter Victor3TM (PerkinElmer precisely) at 570 nm. The cell viability was calculated by normalization to the intensity of the controls. The EC_{50} was calculated by a non-linear curve fit/dose response curve in Origin®[38]. All data represent mean ± standard error of triplicates.

Assay for the Determination of *IC_{50}* with natural Ap_4A

26.7 µL mastermix (8 nM Rv2613c in 20 mM Tris-HCl (pH 8.0), 50 mM NaCl, 1 mM DTT, 0.2 mg/mL BSA, 5 mM NaH_2PO_4, 5 mM $MgCl_2$) and 0.3 µL of inhibitor in DMSO or DMSO as control were mixed and pre-incubated at 25°C for

30 min, followed by addition of 3.0 µL Ap_4A yielding a final concentration of 1 mM. The reaction mixture was mixed thoroughly and incubated for an additional 60 min at 25°C. Rv2613c was inactivated by denaturation at 95°C for 5 min. As additional control 1 mM Ap_4A was incubated in buffer containing 1% DMSO without enzyme. The reaction mixtures were diluted to 80 µL with MilliQ water and the proteins were separated by filtration (Amicon® Ultra- 0.5 mL, centrifugal filter Ultracel®- 10 K) the filter was washed with additional 20 µL of MilliQ water. The samples were analysed by analytical RP-HPLC (4 mm x 30 mm NUCLEODUR® C18 Pyramid 5 µm, Machery and Nagel) with a linear gradient of acetonitrile in 50 mM aqueous triethylammonium acetate (TEAA buffer, pH 7.0). The rate of Ap_4A turnover was calculated relative to the controls. The IC_{50} was calculated by a non-linear curve fit/dose response curve in Origin®[38]. All data represent mean ± standard error of triplicates.

Inhibition of Metabolic Activity of *Mtb*

$2x10^6$ *M. tuberculosis* cells (virulent strain H37Rv) were inoculated in 100 µL LL37 medium (21.8 mg $NaHCO_3$; 2 mM L-glutamine, 20 mL RPMI-1640, 60 mL water) in a 96-well flat bottom microtiter plate. 1 µL of the inhibitors or rifampicin (Sigma Aldrich) were added to yield the final concentrations as indicated (final DMSO concentration: 0.75 %). All samples were performed in triplicates. After incubation for 2 h at 37°C and 5% CO_2, 0.3 µCi ^{3}H-uracil were added per well (0.3 µL ^{3}H-uracil in 2.7 µL LL37 media). The plate was incubated for another 18 h at 37°C and 5% CO_2. *Mtb* was inactivated by treatment with paraformaldehyde (final concentration 4%, in PBS) for 30 min. The cells were harvested with a Inotech Filtermat Harvester 96-well-head onto glas fiber filters (Printed Filtermat A, Perkin Elmer). The filters were washed 3 times with MilliQ water and dried in a microwave at 320 W for 5 min. A sheet of the solid scintillant MeltiLexTMA was molten onto the dry filter at 50°C. Radioactivity was measured using a MicroSenseBeta Counter. The inhibition of the metabolic activity of *Mtb* was calculated by normalization to the intensity of the control of untreated cells. The average of 12 empty wells was subtracted as background from the values before. The Experiment was performed 6 times independently, each time the mean of triplicates was calculated for each sample. The standard deviation (±) was calculated for those six experiments.

ACKNOWLEDGEMENTS

We acknowledge the Screening Center at the University of Konstanz, for professional assistance concerning the high throughput screening. We also thank the AG Scheffner for providing the materials for human cell culture as well as their support concerning human cell culture. For financial support we gratefully acknowledge the DFG and the Konstanz Research School Chemical Biology. S.M.H. also acknowledges the Deutsche Forschungsgemeinschaft, the Studien-stiftung des deutschen Volkes and the Zukunftskolleg of the University of Konstanz for stipends.

ASSOCIATED CONTENT

The Supporting Information is available free of charge on the ACS Publications website at DOI:…..
It includes more detailed Experimental Procedures, 7 additional Figures and one table.

AUTHOR INFORMATION

Corresponding Author

***E-mail:** Andreas.Marx @uni-konstanz.de

The authors declare no competing financial interest.

REFERENCES

1. McLennan, A. G. (1992) *Ap_4A and Other Dinucleoside Polyphosphates* 1ed., CRC Press, Florida.

2. Farr, S. B., Arnosti, D. N., Chamberlin, M. J., and Ames, B. N. (1989) An apaH mutation causes AppppA to accumulate and affects motility and catabolite repression in Escherichia coli, *Proc. Natl. Acad Sci. USA 86*, 5010-5014.

3. Baker, J. C., and Jacobson, M. K. (1986) Alteration of adenyl dinucleotide metabolism by environmental stress, *Proc. Natl. Acad Sci. USA 83*, 2350-2352.

4. Bochner, B. R., Lee, P. C., Wilson, S. W., Cutler, C. W., and Ames, B. N. (1984) AppppA and related adenylylated nucleotides are synthesized as a consequence of oxidation stress, *Cell 37*, 225-232.

5. Johnston, P. A., Archer, B. T., Robinson, K., Mignery, G. A., Jahn, R., and Sudhof, T. C. (1991) rab3A attachment to the synaptic vesicle membrane mediated by a conserved polyisoprenylated carboxy-terminal sequence, *Neuron 7*, 101-109.

6. McLennan, A. G. (2000) Dinucleoside polyphosphates—friend or foe?, *Pharmacol. Ther. 87*, 73-89.

7. Lee, P. C., Bochner, B. R., and Ames, B. N. (1983) AppppA, heat-shock stress, and cell oxidation, *Proc. Natl. Acad Sci. USA 80*, 7496-7500.

8. Mechulam, Y., Fromant, M., Mellot, P., Plateau, P., Blanchin-Roland, S., Fayat, G., and Blanquet, S. (1985) Molecular cloning of the Escherichia coli gene for diadenosine 5',5'''-P1,P4-tetraphosphate pyrophosphohydrolase, *J. Bacteriol 164*, 63-69.

9. Brevet, A., Plateau, P., Best-Belpomme, M., and Blanquet, S. (1985) Variation of Ap4A and other dinucleoside polyphosphates in stressed Drosophila cells, *J. Biol. Chem. 260*, 15566-15570.

10. Goerlich, O., Foeckler, R., and Holler, E. (1982) Mechanism of synthesis of adenosine(5')tetra-phospho-(5')-adenosine (AppppA) by aminoacyl-tRNA synthetases, *FEBS J.126*, 135-142.

11. Guo, R.-T., Chong, Y. E., Guo, M., and Yang, X.-L. (2009) Crystal Structures and Biochemical Analyses Suggest a Unique Mechanism and Role for Human Glycyl-tRNA Synthetase in Ap4A Homeostasis, *J.Biomol.Chem 284*, 28968-28976.

12. Guranowski, A. (2000) Specific and nonspecific enzymes involved in the catabolism of mononucleoside and dinucleoside polyphosphates, *Pharmacol. Ther. 87*, 117-139.

13. Garrison, P. N., Roberson, G. M., Culver, C. A., and Barnes, L. D. (1982) Diadenosine 5',5'''-P1,P4-tetraphosphate pyrophosphohydrolase from Physarum polycephalum. Substrate specificity, *Biochem. J. 21*, 6129-6133.

14. Sassetti, C. M., Boyd, D. H., and Rubin, E. J. (2003) Genes required for mycobacterial growth defined by high density mutagenesis, *Mol. Microbiol. 48*, 77-84.

15. Kisselev, L. L., Justesen, J., Wolfson, A. D., and Frolova, L. Y. (1998) Diadenosine oligophosphates (ApnA), a novel class of signalling

molecules?, *FEBS Lett. 427*, 157-163.

16. Hacker, S. M., Mortensen, F., Scheffner, M., and Marx, A. (2014) Selective Monitoring of the Enzymatic Activity of the Tumor Suppressor Fhit, *Angew. Chem. Int. Ed. 53*, 10247-10250.

17. Hacker, S. M., Welter, M., and Marx, A. (2015) Synthesis of γ-Phosphate-Labeled and Doubly Labeled Adenosine Triphosphate Analogs, *Curr. Protoc. Nucleic Acid Chem. 60, 13.141-13.14.25*

18. Hacker, S. M., Mex, M., and Marx, A. (2012) Synthesis and Stability of Phosphate Modified ATP Analogues, *J. Org. Chem. 77*, 10450-10454.

19. Hacker, S. M., Pagliarini, D., Tischer, T., Hardt, N., Schneider, D., Mex, M., Mayer, T. U., Scheffner, M., and Marx, A. (2013) Fluorogenic ATP Analogues for Online Monitoring of ATP Consumption: Observing Ubiquitin Activation in Real Time, *Angew. Chem. Int. Ed 52*, 11916-11919.

20. Hardt, N., Hacker, S. M., and Marx, A. (2013) Synthesis and fluorescence characteristics of ATP-based FRET probes, *Org. Biomol. Chem. 11*, 8298-8305.

21. Hacker, S. M., Buntz, A., Zumbusch, A., and Marx, A. (2015) Direct Monitoring of Nucleotide Turnover in Human Cell Extracts and Cells by Fluorogenic ATP Analogs, *ACS Chem. Biol. 10*, 2544-2552.

22. Grosdidier, A., Zoete, V., and Michielin, O. (2011) SwissDock, a protein-small molecule docking web service based on EADock DSS, *Nucleic Acids Res. 39*, W270-277.

23. Grosdidier, A., Zoete, V., and Michielin, O. (2011) Fast docking using the CHARMM force field with EADock DSS, *J. Comput.Chem. 32*, 2149-2159.

24. Berthold, M. R., Cebron, N., Dill, F., Gabriel, T. R., Kötter, T., Meinl, T., Ohl, P., Sieb, C., Thiel, K., and Wiswedel, B. (2007) *KNIME: The Konstanz Information Miner ; Studies in Classification, Data Analysis, and Knowledge Organization* Springer.

25. Zhang, J.-H., Chung, T. D. Y., and Oldenburg, K. R. (1999) A Simple Statistical Parameter for Use in Evaluation and Validation of High Throughput Screening Assays, *SLAS Discov. 4*, 67-73.

26. Anderson, M., and Verkman, A. S. (2013) Triazolothienopyrimidine compound inhibitors of urea transporters and methods of using inhibitors, Anderson, M.The Regents of the University of California.

27. Munch, H., Hansen, J. S., Pittelkow, M., Christensen, J. B., and Boas, U. (2008) A new efficient synthesis of isothiocyanates from amines using di-tert-butyl dicarbonate, *Tetrahedron Lett. 49*, 3117-3119.

28. Hansen, J. B., Tagmose, T. M., Mogensen, J. P., Dörwald, F. Z., and Jørgennsen, A. S. (2000) Substituted 3,3-diamino-2-propenenitriles, their preparation and use, (AS, N. N., Ed.), Espacenet.

29. Tagmose, T. M., Zaragoza, F., Boonen, H. C. M., Worsaae, A., Mogensen, J. P., Nielsen, F. E., Jensen, A. F., and Hansen, J. B. (2003) Synthesis and biological activity of 3,3-Diamino-sulfonylacrylonitriles as novel inhibitors of glucose induced insulin secretion from beta cells, *Bioorg. Med. Chem. 11*, 931-940.

30. Mosmann, T. (1983) Rapid colorimetric assay for cellular

growth and survival: Application to proliferation and cytotoxicity assays, *J. Immunol. Methods 65*, 55-63.

31. Kleinpeter, E., Thomas, S., Uhlig, G., and Rudorf, W. D. (1993) Studies of the π-electron distribution in push–pull alkenes by 1H and 13C NMR spectroscopy—II, *Magn. Reson. Chem. 31*, 714-721.

32. Chung, G. A., Aktar, Z., Jackson, S., and Duncan, K. (1995) High-throughput screen for detecting antimycobacterial agents, *Antimicrob. Agents Chemother. 39*, 2235-2238.

33. Yew, W. W., and Leung, C. C. (2006) Antituberculosis drugs and hepatotoxicity, *Respirology 11*, 699-707.

34. Coulson, C. J. (1994) *Molecular Mechanism of Drug Action*, 2nd ed., Taylor & Francis, London.

35. Brun, M. A., Tan, K.-T., Nakata, E., Hinner, M. J., and Johnsson, K. (2009) Semisynthetic Fluorescent Sensor Proteins Based on Self-Labeling Protein Tags, *J.Am. Chem. Soc. 131*, 5873-5884.

36. Schena, A., and Johnsson, K. (2014) Sensing acetylcholine and anticholinesterase compounds, *Angew. Chem. Int. Ed. 53*, 1302-1305.

37. Griss, R., Schena, A., Reymond, L., Patiny, L., Werner, D., Tinberg, C. E., Baker, D., and Johnsson, K. (2014) Bioluminescent sensor proteins for point-of-care therapeutic drug monitoring, *Nat. Chem. Biol. 10*, 598-603.

38. Corporation, O. (1991-2015) Origin, Origin 2015 (64bit) Sr2 ed., OriginLab Corporation, One Roundhouse Plaza PriginLab Coorporation, Northampton MA 01060 USA.